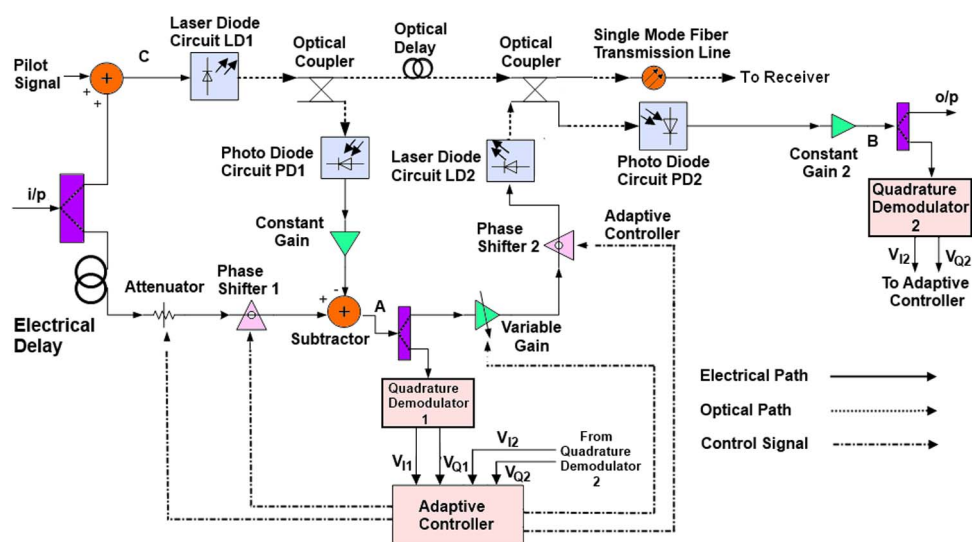# Adaptive Control for Laser Transmitter Feedforward Linearization System

Y. S. Neo
S. M. Idrus
M. F. Rahmat
S. E. Alavi
I. S. Amiri

Adaptive Control for Laser Transmitter Feedforward Linearization System

Y. S. Neo,[1] **S. M. Idrus,**[1] **M. F. Rahmat,**[2] **S. E. Alavi,**[1] **and I. S. Amiri**[3]

[1]Photonic Research Laboratory, Faculty of Electrical Engineering, Universiti Teknologi Malaysia, 81310 Johor, Malaysia
[2]Control & Instrumentation Engineering Department, Faculty of ElectricalEngineering, Universiti Teknologi Malaysia, 81310 Johor, Malaysia
[3]Photonics Research Centre, Department of Physics, Faculty ofScience, University of Malaya, 50603 Kuala Lumpur, Malaysia

Abstract: In this paper, an adaptive control system is employed in a novel implementation technique of the feed forward linearization system for optical analog communication systems' laser transmitter. The adaptive control system applies the Newton trust-region dogleg algorithm, which is a numerical optimization algorithm, to automatically tune the adjustment parameters in the feedforward loops to optimize the feed forward system performance and adapt to process variations. At the end of this paper, significant reductions of over 20 dBm in the third-order inter modulation distortion products have been achieved for operating frequencies from 5.0 to 5.8 GHz.

Index Terms: Adaptive control system, feedforward linearization, laser transmitter, numerical optimization, Newton trust-region dogleg.

1. Introduction

While the current researches of Radio over fiber (RoF) technology is focusing on the millimeter wave frequency range, meaning that external intensity modulation is more prevalent nowadays, direct modulation of laser diode at lower frequencies such as the ISM band is still an interested subject because of its simplicity and cost effectiveness [1], [2]. However, in the direct modulation of a laser diode, the dynamic range of the optical fiber links is limited by the nonlinear distortions generated by laser nonlinearities [3]–[5]. Feedforward linearization is an effective technique for laser nonlinearity compensation system because of its ability to provide broadband distortion reduction at high frequencies, and reductionin all order of distortions regardless of the laser nonlinear characteristics [6]–[11]. However, feedforward is also a complicated and sensitive scheme as itinvolves cancellation between 2 signals of almost equal in magnitude and phase. In order to achieve optimumcancellation, optimizations are needed for the control parameters in the feedforward loops. Furthermore, changing operating conditions or process variations may disrupt the path matching and loop balance [12], [13], which causes the system performance to degrade in real time applications. Hence, the feedforward linearization system needs
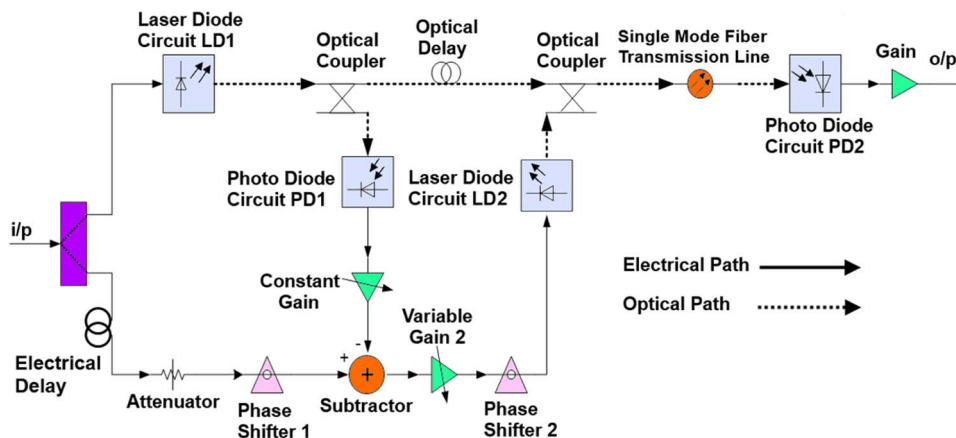
Fig. 1. Block diagram of feedforward linearization system.

to be incorporated with adaptive properties in order to maintain its performance for more practical implementations. This work demonstrates a novel design of feedforward linearization system for optical analog communication systems' laser transmitter equipped with an adaptive control system. Pilot signals are used to guide the adaptation process and the quadrature detection method is used to detect the pilot signal levels at the output of the feedforward loops. The adaptive controller performs the Newton trust region dogleg algorithm, which is a robust algorithm for equation solving, to simultaneously minimize the in-phase and quadrature signal levels at the quadrature detector output. The Newton method provides rapid convergence to the solution point, butthis method is dependent on the initial guess [14]. The trust region method enhances the Newton method to become more globally convergent by defining a region where the Newton model is trusted to be a good enough representation of the objective function [15]. Furthermore, the dogleg method ensures the reduction in objective function for each iteration by using the combination of the steepest descent step and Newton step to approximate the optimal trajectory within the trust region [16].

This paper proceeds as follows. Section 2 discusses the feedforward system and the architecture of adaptive feedforward system. The mathematical analysis of the feedforward loops are done in Section 3 and the adaptive control algorithm is discussed in Section 4. Sections 5 and 6 show the system setup and results of the developed model, respectively. Finally, Section 7 concludes this paper.

2. Architecture of the Designed System

Fig. 1 shows the block diagram of a laser transmitter feedforward linearization system. The system consists of 2 loops, where the inner loop is signal cancellation loop and the outerloop is error cancellation loop. The role of the signal cancellation loop is to acquire the distortions from the primary laser diode (LD1). On the other hand, the role of the error cancellation loop is to cancel the distortions from LD1 with the distortion signal obtained from the signal cancellation loop. As the system involves cancellation between 2 signals of almost equal in terms of magnitude and phase, the magnitude and phase parameters in both loops have to be well adjusted so that the 2 signal match each other. In both the signal cancellation and error cancellation loop, there are variable attenuator/amplifier and phase shifters which are responsible for amplitude matching and phase matching, respectively.

In an adaptive feedforward system, the signals from the chosen observation points in the open loop feedforward system are used to extract the error signals. The error signals are then minimized by iteratively updating the amplitude and phase adjustment parameters of the system in order to achieve adaptation. The architecture of the proposed adaptive feedforward system of this project is shown in Fig. 2 Compared to the open loop feedforward linearization system in
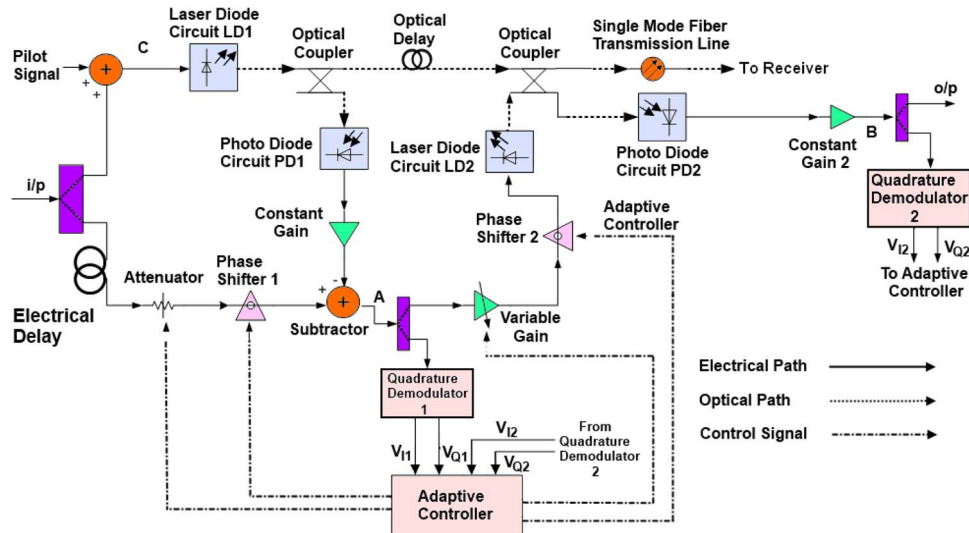
Fig. 2. Block diagram of the adaptive feedforward linearization system.

Fig. 1, there is quadrature demodulators at the output of the signal cancellation loop and error cancellation loop. A pilot signal has also been inserted at the input of laser LD1.

From the block diagram, point A and point B are chosen as the observation points for the signal cancellation loop andthe error cancellation loop respectively. The adaptations for each of the loop are guided by a different pilot signal. For the signal cancellation loop, one of the input carrier signals can be used as the pilot signal. As for the error cancellation loop, the pilot signal is inserted at point C, the input of the first laser diode (LD1) along with the input carrier signals. The inserted pilot signal should be about the same level with the IMD3 products but different in-frequency. The level of the pilot signals at point A and point B is detected by quadrature demodulators using the quadrature detection method. The local oscillators (LO) for each of the quadrature detectors are tuned to the corresponding pilot signal frequencies for their respective loops to perform direct conversions. Both the in-phasesignal and quadrature signal of the quadrature detectors are given as $V_I = (1/2)A\cos\phi$, and $V_Q = (1/2)A\sin\phi$, respectively, where A is the magnitude of the pilot signal and ϕ is the phase difference between the pilot signal and the LO of the quadrature detectors. Both the in-phase signal and quadrature signal of the quadrature detector are then fed to the adaptive controller to become error signals. The adaptive controller will perform control algorithms to adjust thegains and phase shifts in the feedforward loop in order to minimize the in-phase signal and quadrature signal.

3. Mathematical Analysis for the Feedforward Loops

Fig. 3 shows the complex baseband representation of the proposed feedforward linearization system. V_{in} is the input carrier signal, V_p is the pilot signal, and V_{out} is the output signal. In the signal cancellation loop, the first laser diode (LD1) has a laser current to optical power conversion gain of L_1 and introduces a phase shift of α, which constitutes a complex gain of $L_1 < \alpha$. V_d is the total of distortion terms introduced by LD1. D_1 and G_1 are the gains of photodetector 1 and the constant gain 1 respectively. In the lower branch of the cancellation loop, $1/A_1$ and θ_1 are the attenuation and phase shift for the variable attenuator and phase shifter 1 respectively.

In the error cancellation loop, there are A_2 and θ_2 which are the gain and phase shift for the variable amplifier and phase shifter 2 respectively. L_2 and β are the gain and phase shift introduced by the second laser diode (LD2) respectively. As the input signal of LD2 is small, it is assumed to be operating linearly [17]. Hence, no additional distortion term is added to LD At the
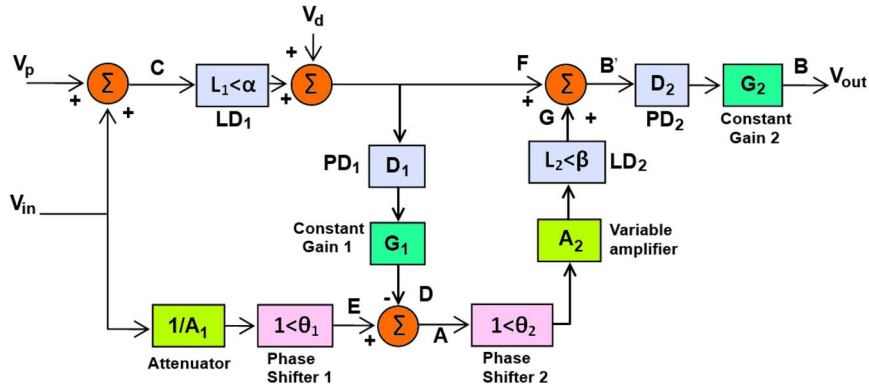
Fig. 3. Simplified schematic diagram of the feedforward linearization system.

output of the error cancellation loop, there are D_2 and G_2 which represent the gains for photodetector 2 and constant gain 2, respectively.

If A_1 and θ_1 are well adjusted such that $A_1 = D_1 G_1 L_1$ and $\theta_1 = \alpha$, the output of the signal cancellation loop, S_A will contain only the distortion and the pilot signal

$$S_A = -D_1 G_1 L_1 \angle \alpha_p - D_1 G_1 V_d. \tag{1}$$

On the other hand, if A_2 and θ_2 are well adjusted such that $A_2 = 1/D_1 G_1 L_2$ and $\theta_2 = -\beta$, the pilot signal and the distortion term from LD1 will be cancelled all together, leaving only the desired input carrier signal at the output of the system, S_B, which is given by

$$S_B = D_2 G_2 L_1 \angle \alpha \times V_{in}. \tag{2}$$

Now, the output of the quadrature demodulators located at point A and B are being seen. The first quadrature detector (QD1) will be taking the signal from point A, S_A. The input carrier signal itself is chosen as the pilot signal to guide the adaptation of the signal cancellation loop. If we let the phase of the LO in QD1 be γ_1 the in-phase output signal of QD1, V_{I1} is given by

$$V_{I1} = \frac{1}{2}|V_{in}|A_1 \cos(\theta_1 - \gamma_1) + \frac{1}{2}|V_{in}|D_1 G_1 L_1 \cos(\alpha - \gamma_1). \tag{3}$$

where $|V_{in}|$ is the magnitude of V_{in}. On the other hand, the quadrature output signal of QD1, V_{Q1} is given by

$$V_{Q1} = \frac{1}{2}|V_{in}|A_1 \sin(\gamma_1 - \theta_1) + \frac{1}{2}|V_{in}|D_1 G_1 L_1 \sin(\gamma_1 - \alpha). \tag{4}$$

In order to achieve adaptation, both V_{I1} and V_{Q1} have to be minimized in terms of their magnitude. This is true only if $A_1 = D_1 G_1 L_1$ and $\theta_1 = \alpha$, which is identical to the conditions for (1). Equating (3) and (4) to 0:

$$\begin{pmatrix} A_1 \cos(\theta_1 - \gamma_1) + D_1 G_1 L_1 \cos(\alpha - \gamma_1) \\ A_1 \sin(\gamma_1 - \theta_1) + D_1 G_1 L_1 \sin(\gamma_1 - \alpha) \end{pmatrix} = \begin{pmatrix} 0 \\ 0 \end{pmatrix}. \tag{5}$$

As for the error cancellation loop, the second quadrature detector (QD2) will be taking the signal from point B, S_B. The pilot signal, V_p is the signal to be detected. Let the phase of the LO in Q0D2 be γ_2. The in-phase output of QD2, V_{I2} is given by

$$V_{I2} = \frac{1}{2}D_2 G_2 L_1 |V_p| \cos(\alpha - \gamma_2) - \frac{1}{2}D_1 G_1 L_1 D_2 G_2 A_2 L_2 |V_p| \cos(\theta_2 + \beta + \alpha - \gamma_2) \tag{6}$$

where $|V_p|$ is the magnitude of V_p. On the other hand, the quadrature output of QD2, V_{Q2} can be obtained as

$$V_{Q2} = \frac{1}{2}D_2 G_2 L_1 |V_p| \sin(\gamma_2 - \alpha) - \frac{1}{2}D_1 G_1 L_1 D_2 G_2 A_2 L_2 |V_p| \sin(\gamma_2 - \theta_2 - \beta - \alpha). \tag{7}$$

Similar to the signal cancellation loop, V_{I2} and V_{Q2} have to be minimized in terms of their magnitude, which is true only if $A_2 = 1/D_1 G_1 L_2$ and $\theta_2 = -\beta$. These are identical to the conditions for Equation (2). Equating (6) and (7) to 0:

$$\begin{pmatrix} D_2 G_2 L_1 \cos(\alpha - \gamma_2) - D_1 G_1 L_1 D_2 G_2 A_2 L_2 \cos(\theta_2 + \beta + \alpha - \gamma_2) \\ D_2 G_2 L_1 \sin(\gamma_2 - \alpha) - D_1 G_1 L_1 D_2 G_2 A_2 L_2 \sin(\gamma_2 - \theta_2 - \beta - \alpha) \end{pmatrix} = \begin{pmatrix} 0 \\ 0 \end{pmatrix}. \tag{8}$$

The adaptation process for the signal cancellation loop and error cancellation loop is equivalent to solve for (5) and (8), respectively. As the parameters for both of the equations aremostly unknown in real time applications, the adaptive controller has to perform numerical optimization algorithms to solve the equations by iterations.

4. Control Algorithm

In the section above, the modeling of optimization problem for the adaptation process has been done in which the objective function and variables for the optimization problem has been identified. Referring back to Fig. 2, the objective functions of the problem are the outputs of QD1 and QD2. The variables of the objective functions are the amplitude and phase matching parameters in the feedforward loops. The goal of the problem is to minimize the value of the objective functions which represent the levels of the pilot signals. The algorithm that is used in this paper is the trust region dogleg Newton's method. This method is chosen because it has good convergence properties in equations solving and provides more robustness [18].

The algorithm is programmed and embedded in the adaptive controller block shown in Fig. 2. In the Newton trust region dogleg method, the Jacobian matrix of the equations to be solved is needed, but in the application here the Jacobian matrix is not defined explicitly. Hence, it has to be computed using finite difference approximation [19]. Each of the iterations in the adapting process is made up of three stages, where the first and second stages involve adding small increments to the magnitude and phase parameter respectively. With the information of the partial derivatives from the first and second stages, the Jacobian matrix can be calculatedin the third stage. Then, the Jacobian matrix is used to compute the trial step using the dogleg method.

The Newton trust region dogleg method attempts to minimize a Newton model representation of the objective function rather than the original one, within the trust region. The Newton model function is given as [18]

$$\begin{aligned} m(d) &= \frac{1}{2}\|F(x) + J(x)d\|_2^2 \\ &= \frac{1}{2}F(x)^T F(x) + d^T J(x)^T F(x) + \frac{1}{2}d^T J(x)^T J(x)d \end{aligned} \tag{9}$$

where d is the step taken, x is the variable, $F(x)$ is the original objective function, and $J(x)$ is the Jacobian matrix for $F(x)$. The subproblem for each iteration is given as

$$\min_d m_k(d) = \frac{1}{2}F(x_k)^T F(x_k) + d^T J(x_k)^T F(x_k) + \frac{1}{2}d^T J(x_k)^T J(x_k)d \tag{10}$$

subject to $\|d\| \le \Delta_k$ where k is the iteration number, and Δ_k is the trust region radius. The dogleg method approximates the curve trajectory of the minimum point using the combination of the Cauchy step, d_c, which is along the steepest descent direction, and the Newton step

TABLE 1

Laser Parameters of the Primary and Secondary Laser Diodes

Parameters	Value	Unit
Active layer volume	1×10^{-16}	m^3
Photon lifetime	3×10^{-12}	s
Carrier lifetime	1×10^{-9}	s
Carrier density at transparency	$1 \times 10^{+24}$	m^{-3}
Gain coefficient	2.125×10^{-12}	$m^3\,s^{-1}$
Mode confinement factor	0.4	-
Spontaneous emission factor	3×10^{-5}	-
Gain compression coefficient	5×10^{-23}	m^3
Threshold current	22.3	mA

$d_n = -J_k^{-1}F_k$. The Cauchy step and the trajectory for the step which is also known as the dogleg path, $d(\tau)$ is given by [18]

$$d_c = \frac{a_k \Delta_k}{\|J_k^T F_k\|} \cdot J_k^T F_k, \quad a_k = \min\left\{1, \frac{\|J_k^T F_k\|^3}{\Delta_k F_k^T J_k (J_k^T J_k) J_k^T F_k}\right\} \tag{11}$$

$$d(\tau) = \begin{cases} \tau d_C, & 0 \leq \tau \leq 1 \\ d_C + (\tau - 1)(d_N - d_C), & 1 \leq \tau \leq 2 \end{cases} \tag{12}$$

where τ is to be determined by the intersection point of the trust-region boundary and the dog-leg path. In order to find τ, the following quadratic equation has to be solved:

$$\|d_C + (\tau - 1)(d_N - d_C)\|^2 = \Delta_k^2. \tag{13}$$

The trial step can be obtained by substituting τ in Equation (13). Next, the ratio of the Newton model reduction to the actual reduction is computed to decide on whether to accept or reject the step. The trial step will be rejected if a negative value is obtained, and it will be recalculated with a smaller trust-region radius. Otherwise, the trial point becomes the current point. The adapting process stops when the parameters are within 0.01 near the optimal point.

5. System Setup

The primary and secondary laser diodes (LD1 and LD2) in the system model are modeled using laser rate equations, where the effects of gain compression and relaxation oscillation have been included. The parameters of the model are listed in Table 1. Both the laser diodes are biased at 38 mA with mean optical output power of 2 mW (3 dBm), and modulation peak currents of 16 mA. Laser LD1 has an optical wavelength of 1550 nm. Laser LD2 has the same specifications as LD1, except that laser LD2 operates at 1548 nm. Both the laser diodes have to be separated by at least 0.5 nm in optical wavelength to avoid optical beating. In practical measurements, LD1 and LD2 do not have to be identical, but it is important for LD2 to be operated in the linear region. The setup is including the PIN diode controlled phase shifter which is able to maintain its amplitude response over a few gigahertzes to adjust the phase shift parameters. Microprocessor is used as the platform to implement the adaptive control algorithm. The systemis setup at frequency 5.2 GHz, which is the operating frequency for IEEE 802.11a Standard used in wireless local area network (WLAN) communication. The input signal is a 2-tone test signal at 5.2 GHz with 10 MHz frequency spacing. Theamplitude of the input signal is 1 a.u. (arbitrary unit) with reference to the modulation peak current.

The actual laser current to optical power conversion gain and laser output phase shift of the laser diode are unknown, and they usually vary with different operating frequencies and input current levels. In order to optimize the performance of the feedforward linearization system, the system is repeatedly tested with an iterated variation of the loop adjustment parameters, which is done by sweeping the parameters. The optimization of the parameters is done bynested
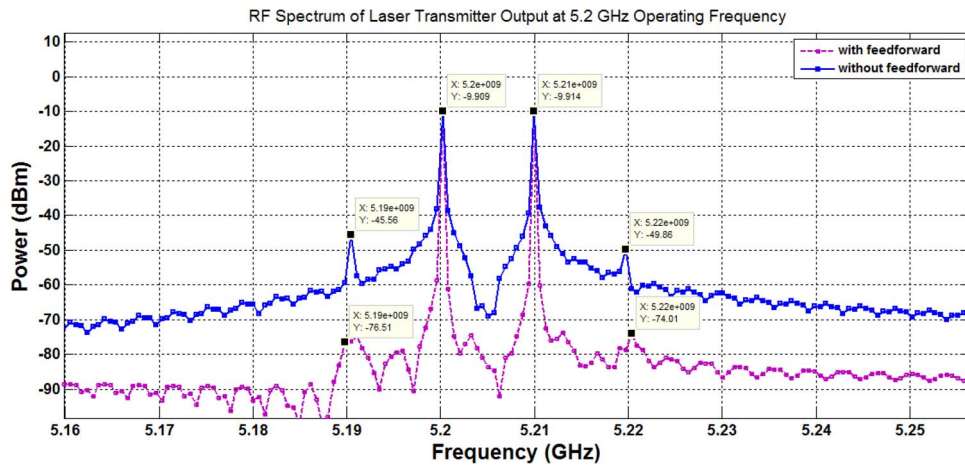
Fig. 4. RF spectrum with and without feedforward linearization.

parameters sweeping in which the result is inspected manually and the parameter values are also changed manually. It takes many trials to achieve the best performance and it is also a time consuming procedure.

6. Results and Discussion

The adaptive controller managed to find the optimum control parameter values for both the signal cancellation loopand error cancellation loop in nine and eight iterations, respectively. This also means that 28 and 25 function evaluations are needed for the signal cancellation loop and error cancellation loop respectively, by taking into account the computation of the Jacobian matrix for each iterations. While in the real-time, the required settling time can be obtained by multiplying the number of function evaluations with the sampling time of the controller.

Fig. 4 shows the RF spectrum of the output of laser transmitter with and without feedforward linearization. The frequencies of the 2-tone test signal are known as f_1 and f_2, with the value 5.20 GHz and 5.21 GHz respectively. Meanwhile, the first IMD3 product $IMD3_{2f1-f2}$ and the second IMD3 product $IMD3_{2f2-f1}$ are at 5.19 GHz and 5.22 GHz respectively. From the RF spectrum, it can be seen that the suppression in $IMD3_{2f1-f2}$ is 30.95 dB, while the suppression in $IMD3_{2f2-f1}$ is 24.15 dB. The output of the laser transmitter without feedforward linearization has broaden spectra due to the presence of IMD products near the fundamental tones which affects the computation of RF spectrum for frequencies at the closest proximity of the fundamental tones. With the IMD products being suppressed, the spectrum of the fundamental tones becomes narrower and more distinguished as a result, as illustrated in the output RF spectrum of laser transmitter with feedforward linearization.

The open loop laser transmitter feedforward linearization system is also tested with varying operating frequency from 5.0 GHz to 5.8 GHz. The adjustment parameters in the system remain unchanged as at the frequency 5.2 GHz. This measureis to look at on the effect of frequency variation on the system performance. The reductions in the IMD3 products for each frequency are then computed and plotted against the operating frequencies. The plot is shown in Fig. 5.

The plot shows that the system performance is frequency dependent. The reductions for both IMD3 products are maximumat 5.2 GHz operating frequency, where the adjustment parameters are optimized. As the operating frequency moves furtheraway from 5.2 GHz, the IMD3 reductions fall gradually. The reductions for both IMD3 products fall below 10 dB atfrequency 5.8 GHz. Since the electrical components in the feedforward loops such as attenuator and variable amplifier have their own frequency response, they behave differently as the frequency changes. Therefore, when the operating frequency changes while the same adjustment parameters are used, the system performance will drop.
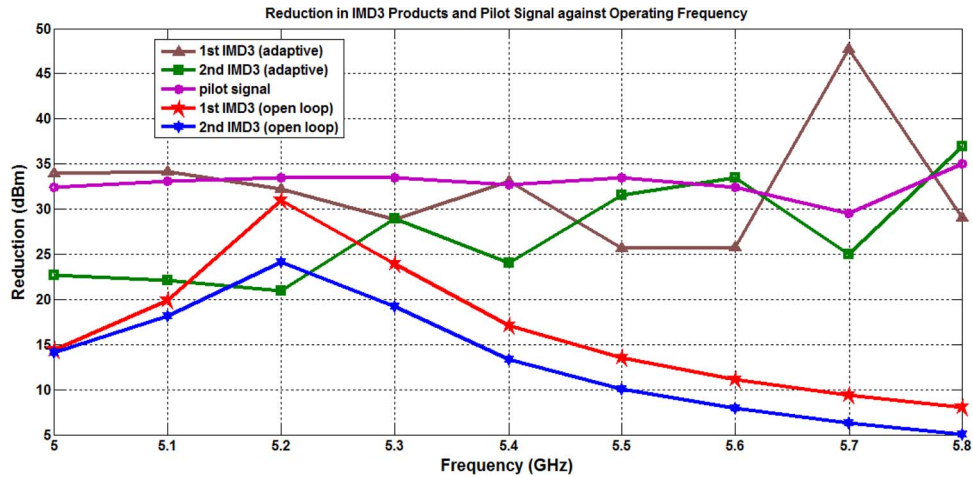
Fig. 5. Reduction in IMD3 products for open loop feedforward linearization and adaptive feedforward linearization system (with Pilot Signal) against operating frequency.
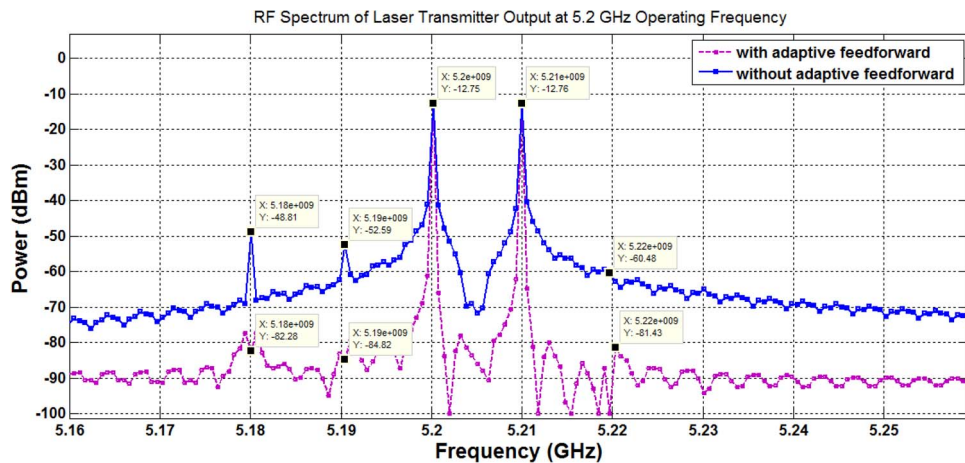

Fig. 6. RF spectrum with and without adaptive feedforward linearization.

Next, Fig. 6 shows the RF spectrum of the laser transmitter output with andwithout adaptive feedforward linearization system at operating frequency 5.2 GHz. The difference between this RF spectrum and the one in Fig. 4 is the introduction of a pilot signal at the frequency 5.18 GHz. It should be noted that the pilot signal has been lowered by 2 orders of magnitude compared to the fundamental signals in order to avoid from introducing more IMD products. For the laser with adaptive feedforward linearization system, the suppression in $IMD3_{2f1-f2}$ is 32.23 dB and 20.95 dB for $IMD3_{2f2-f1}$. Meanwhile, the pilot signal has also been suppressed by 33.47 dB. The comparison of IMD3 reduction for the feedforward linearization system with and withoutadaptive control is presented in Table 2.

It is observed that the reduction has shown an increase of 1.28 dB for the first IMD3 but a decrease of 3.2 dB for the second IMD3. This discrepancy in performance is expected since the magnitude and phase matching for error cancellation are different for each frequencies. While the pilot signal is the only objective of minimization, the other distortion products are expected to be cancelled differently. The results prove that the adaptation process of the feedforward linearization system has been successful. The adjustment parameters in the feedforward loops are well adjusted that the system has delivered significant reduction in the distortion products.

Other than that, the performance of the adaptive feedforward linearization system is also tested by varying the operating frequency from 5.0 GHz to 5.8 GHz. As the electrical

TABLE 2

Comparison of IMD3 reductions with and without adaptive control

	Without adaptive (dB)	With adaptive (dB)
1st IMD3	30.95	32.23
2nd IMD3	24.15	20.95

components in the system will undergo parameter drifts asthe frequency changes, by varying the operating frequency the adaptive feedforward linearization system can be tested for its immunity towards parameter drifts. As the operating frequency shifted from the optimized frequency 5.2 GHz to the next frequency such as 5.1 GHz or 5.3 GHz, it takes two iterations (7 function evaluations) for the algorithm toconverge to the new optimum values for each of the signal cancellation loop and the error cancellation loop. The same istrue for frequency shifting from 5.3 to 5.4 GHz, 5.4 to 5.5 GHz and so on. Fig. 5 shows the plot of reductions in the IMD3 products and the pilot signal against the operating frequency, overlaying with the IMD3 reductions of open loop feedforward linearization system.

From the plot, it is observed that the reduction of the pilot signal level is consistently above 30 dB, while thereductions for the IMD3 products fluctuate with operating frequencies. However, they seldom drop lower than 25 dB andall of them are well above 20 dB. It is observed that there is a big jump at frequency 5.7 GHz as the reduction for the first IMD3 product suddenly rises to 47.78 dB. It is expected that the optimum matching of magnitude and phase for the error cancellation loop has occurred at this frequency. This shows that as the operating frequency varies, the developed adaptive feedforward linearization system is still able to contribute significant distortion reductions.

As shown in Fig. 5, the open loop feedforward linearization system encounters performance degradation under parameter drift as expected. While the system performance can be restored by reoptimizing the loop parameters, it is hard to be achieved by human surveillance, because it would take many sweep iterations to obtain the optimal parameters for each of the frequencies. On the other hand, the developed adaptive feedforward linearization system can find the optimal parameters for each frequency by automatically updating the parameters until the minimum pilot signal level is achieved. Also in Fig. 5, it is shown that the reduction in IMD3 products and pilot signal have been maintain well above 20 dB, which indicates that the effect of frequency variation has been alleviated.

7. Conclusion

In this paper, a laser transmitter adaptive feedforward linearization system has been developed. The open loop laser transmitter feedforward linearization system has shown that it can achieve significant reduction in the IMD3 products. However, the manual tuning of the loop adjustment parameters in the system is time consuming and impractical. In addition to that, the system performance is also strongly influenced by parameter drifts. On the other hand, the addition of an adaptive control system has effectively simplified the task of adjusting the parameters and substantially reduced the number of sweep iterations needed. The adaptive control system has also successfully stabilized the system performance in the case of parameter drifts. As a result, the laser transmitter feedforward linearization system has now been upgraded and it becomes more suitable for practical implementations.

References

[1] P. Assimakopoulos, A. Nkansah, N. J. Gomes, and D. Wake, "Statistical distribution of EVM measurements for direct-modulation radio-over-fiber links transporting OFDM signals," *IEEE Trans. Microw. Theory Tech.*, vol. 61, no. 4, pp. 1709–1717, Apr. 2013.

[2] M. Faugeron *et al.*, "High optical power, high gain and high dynamic range directly modulated opticallink," *J. Lightw. Technol.*, vol. 31, no. 8, pp. 1227–1233, Apr. 2013.

[3] V. J. Urick *et al.*, "Long-haul analog photonics," *J. Lightw. Technol.*, vol. 29, no. 8, pp. 1182–1205, Apr. 2011.

[4] C. Lim *et al.*, "Fiber-wireless networks and subsystem technologies," *J. Lightw. Technol.*, vol. 28, no. 4, pp. 390–405, Feb. 2010.

[5] J. Yao, "Microwave photonics," *J. Lightw. Technol.*, vol. 27, no. 3, pp. 314–335, Feb. 2009.

[6] L. S. Fock and R. S. Tucker, "Reduction of distortion in analogue modulated semiconductor lasers by feedforward-compensation," *Electron. Lett.*, vol. 27, no. 8, pp. 669–671, Apr. 1991.

[7] D. Hassin and R. Vahldieck, "Feedforward linearization of analog modulated laser diodes—Theoretical analysis and experimental verification," *IEEE Trans. Microw. Theory Tech.*, vol. 41, no. 12, pp. 2376–2382, Dec. 1993.

[8] T. Ismail, L. Chin-Pang, J. E. Mitchell, and A. J. Seeds, "High-dynamic-range wireless-over-fiber link using feedforward linearization," *J. Lightw. Technol.*, vol. 25, no. 11, pp. 3274–3282, Nov. 2007.

[9] S. R. O'Connor, T. R. Clark Jr., and D. Novak, "Wideband adaptive feedforward photonic link," *J. Lightw. Technol.*, vol. 26, no. 15, pp. 2810–2816, Aug. 2008.

[10] H. Cheung, I. Robertson, V. Postoyalko, and S. Iezekiel, "Nested loop feedforward linearization of directly modulated laser diode," in *Proc. MWP*, 2009, pp. 1–4.

[11] D. Novak, T. Clark, S. O'Connor, D. Oursler, and R. Waterhouse, "High performance, compact RF photonic transmitter with feedforward linearization," in *Proc. MILCOM*, 2010, pp. 880–884.

[12] S. Kang, M. Song, H. Yi, and S. Hong, "Adaptive control method for a feedforward amplifier," in *Proc. IEEE 59th VTC—Spring*, 2004, pp. 1182–1186.

[13] Z. Wang, K. Qin, K. Yang, M. Zhu, C. Chen, and X. Zhang, "An adaptive control method for microwave linear power amplifier," in *Proc. Int. Conf. Commun., Circuits Syst.*, 2006, pp. 2573–2576.

[14] E. K. P. Chong and S. H. Zak, *An Introduction to Optimization*. New York, NY, USA: Wiley, 1996.

[15] Y.-X. Yuan, "A review of trust region algorithms for optimization," in *Proc. 4th ICM*, J. M. Ball and J. C. R. Hunt, eds., 2000, pp. 271–282.

[16] T. Steihaug, "The conjugate gradient method and trust regions in large scale optimization," *SIAM J. Numer. Anal.*, vol. 20, no. 3, pp. 626–637, 1983.

[17] B. Buxton and R. Vahldieck, "Noise and intermodulation distortion reduction in an optical feedforward transmitter," in *Proc. IEEE MTT-S Int. Microw. Symp.*, 1994, pp. 1105–1108 vol. 2.

[18] J. Nocedal and S. Wright, *Numerical Optimization*. New York, NY, USA: Springer-Verlag, 2006.

[19] W. Sun and Y.-X. Yuan, *Optimization Theory and Methods: Nonlinear Programming*. New York, NY, USA: Springer-Verlag, 2006.